Ab Initio Investigation of the Structures and Properties of Polyaminoborane

Denis Jacquemin,*,† Eric A. Perpète,† Valérie Wathelet, and Jean-Marie André

Laboratoire de Chimie Théorique Appliquée, Facultés Universitaires Notre-Dame de la Paix, rue de Bruxelles, 61, B-5000 Namur, Belgium

Received: August 4, 2004

We have investigated the structures and the properties of polyaminoborane oligomers by using ab initio computational tools including dynamic electron correlation effects. It turned out that the PBE0/6-31G(2d) method provides a good agreement between experimental and theoretical structures. The key data include geometries, rotational profiles, infrared spectra, vertical excitation energies, atomic charges, and dipole moments. The variations of these properties upon conformation changes are studied. Our results are compared to available experimental measurements.

Introduction

Polyaminoborane (PAB, Figure 1), an inert white solid, has been synthesized by different groups using various physical or chemical procedures.[1−10] Recently Nöth and Thomas[11] and the Manners group[12−15] have obtained relevant information about the structures of PAB dimers synthesized by rhodium-catalyzed dehydrocoupling. The catalytic dehydrocoupling procedure described in ref 12 is not able to provide polymeric PAB due to fast backbiting of the growing chain.[12] Probably due to the partially/mainly amorphous nature of the synthesized polymer, little is known about the properties of long PAB chains. The only available data are some IR,[1,3−5,9] X-ray photoelectron spectroscopy (XPS),[10] and solid-state NMR spectra.[5,6] In this contribution, we have used theoretical tools to investigate the properties of unsubstituted PAB, determining stable conformations, charges, excitation energies, vibrational spectra, and so forth. This allows us, on one hand, to confirm/contradict some of the experimental assumptions and, on the other hand, to provide results that would help in determining the structure of PAB, if the crystallinity of the polymer was improved. To our knowledge, with the exception of two previous works dealing with the all-trans conformers,[16,17] this is actually the first theoretical investigation of long PAB oligomers, although results for small chains do exist (see, for instance, ref 18 and references therein).

I. Computational Details

For our investigations, we have selected the Hartree−Fock (HF) approach, the second-order Møller−Plesset (MP2) scheme, and three hybrid-DFT (B3LYP,[19] B98,[20] and PBE0[21]) functionals. Various Pople polarized split-valence basis sets have been tested: 6-31G(d), 6-31G(2d), 6-31G(d,p), 6-311G(d), 6-311G(2d), 6-311G(3d), 6-311G(2df), and 6-311G(3df). Basis sets including diffuse functions have been considered as well: 6-31+G(2d), 6-311+G(d), 6-311+G(2d), 6-311++G(2d), 6-311++G(2d,p), 6-311++G(3d,p), and 6-311+G(2df,p). Test calculations have been performed with Dunning's double-ζ and triple-ζ basis sets (cc-pVDZ and cc-pVTZ) including one or two sets of diffuse functions (*aug*-cc-pVDZ and *d-aug*-cc-pVDZ). In the following, two techniques have been proved to lead to the "optimal" results: PBE0/6-31G(2d) [or 6-31+G(2d)] and MP2/6-311G(2d). Indeed, the agreement between the PBE0/6-31G(2d) geometries and X-ray structures is very good for small PAB oligomers whereas MP2/6-311G(2d) provides converged theoretical results for most of the properties (section II.A). All the calculations have been performed for PAB oligomers (Figure 1) with Gaussian 03[22] by using the following procedure:

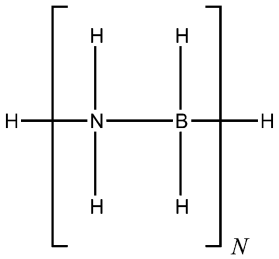

Figure 1. Illustration of polyaminoborane oligomers.

1. Geometry Optimization. The ground-state geometry of each oligomer (Figure 1[23]) has been determined by a full optimization of its structural parameters. These minimizations have been performed until the rms (root-mean-square) residual force is lower than 1×10^{-6} au (this corresponds to the *verytight* threshold in Gaussian 03) when the geometries are used for vibrational spectra calculations. In the other cases, the *tight* threshold (rms residual forces lower than 1×10^{-5} au) has been used. At the PBE0 level, the geometries have been determined by using an *ultrafine* integration grid [pruned (99,590) grid,[24]], except for the values reported in Table 1 [default *fine* pruned (75,302) grid]. The rotational profiles have been obtained by fixing one coordinate (the adhoc dihedral angle) and then optimizing all the other parameters.

2. Vibrational Spectra. The vibrational frequencies and the related intensities have been determined by a fully analytic determination of the Hessian. Experimental-looking spectra have been obtained by convoluting the theoretical results, using a mixed Lorentzian (80%)/Gaussian (20%) function with two different full width at half-maximum values (fwhm[25] = 5 and 25 cm^{-1}). At the PBE0 level, the Hessian calculation as well as the preceding geometry optimizations have been performed

* To whom correspondence should be addressed. E-mail: denis.jacquemin@fundp.ac.be.

† Research Associate of the Belgian National Fund for Scientific Research.

10.1021/jp0465027 CCC: $27.50
Published on Web 10/08/2004

TABLE 1: Comparison between the Theoretical and the Experimental Parameters of Molecules I, II, and III Sketched in Figure 2 (and Figures 1−3 of Reference 12)[a]

parameter	X-ray (ref 12)	HF/6-31G(2d)	B3LYP/6-31G(2d)	B98/6-31G(2d)	PBE0/6-31G(2d)	MP2/6-311G(2d)
			molecule **I**			
d_{B-N}	1.595−1.596	1.606	1.609	1.607	1.599	1.602
d_{N-C}	1.474−1.478	1.464	1.476	1.476	1.464	1.468
α_{B-N-B}	86.3	86.6	86.6	86.5	86.3	86.9
α_{N-B-N}	93.7	93.4	93.4	93.5	93.7	93.1
α_{C-N-C}	109.0	109.6	109.4	109.5	109.7	109.5
α_{B-N-C}	115.4−115.6	114.8	114.9	114.9	114.8	114.8
			molecule **II**			
d_{N-B}	1.584−1.600	1.594−1.609	1.596−1.611	1.594−1.610	1.587−1.601	1.590−1.604
d_{N-C}	1.471−1.485	1.471	1.485	1.485	1.473	1.476
α_{B-N-B}	86.6−86.7	86.7	86.8	86.7	86.6	87.5
α_{N-B-N}	93.1−93.5	93.3	93.2	93.3	93.4	92.5
α_{C-N-C}	101.8	103.0	102.9	103.0	103.0	102.3
α_{B-N-C}	116.7−118.3	116.3−117.5	116.3−117.6	116.3−117.5	116.1−117.8	115.7−118.1
			molecule **III**			
$d_{N(1)-B(1)}$	1.595	1.633	1.622	1.618	1.607	1.607
$d_{N(2)-B(1)}$	1.576	1.579	1.582	1.581	1.573	1.571
$d_{N(2)-B(2)}$	1.598	1.641	1.629	1.625	1.614	1.617
d_{N-C}	1.494−1.502	1.481−1.487	1.494−1.502	1.493−1.501	1.481−1.488	1.486−1.493
α_{B-N-B}	111.4	111.5	111.5	111.4	111.2	111.6
α_{N-B-N}	112.7	110.0	108.4	108.2	108.7	107.5
α_{C-N-C}	101.8−104.0	102.6−103.8	102.3−103.6	102.4−103.6	102.4−103.5	101.7−103.0
α_{C-N-B}	109.9−114.9	107.0−115.5	107.5−115.2	107.4−115.2	107.4−114.9	110.9−114.9

[a] The point groups are D_{2h}, C_{2h}, and C_1, respectively. Bond lengths are in Å, and valence angles in degrees.

with an *ultrafine* integration grid. Indeed, this grid is recommended to accurately optimize geometries and to produce correct frequencies for all vibrational modes. The usual scaling factor has been used to reduce the residual discrepancy between the computed frequencies and the experimental values.[26−29]

3. Charges and Dipole Moment. Among the several methods available to describe partial atomic charges in a molecule, we have selected an electrostatic-potential-derived formalism, the Merz−Kollman procedure (so-called MK or ESP charges).[30] It yields charges which are consistent with the experimental data.[31] Test calculations using the CHELPG scheme[32] have been performed as well. The norm of the dipole moment ($|\mu|$) has been obtained by the standard expectation value formula.

4. Excitation Energies. We have computed the singlet-state excitation energies with the time-dependent density functional theory (TDDFT)[33] as implemented in Gaussian 03, with the B3LYP and PBE0 functionals. This procedure provides excitation energies that are comparable with the experimental results (see, for instance, ref 34−39 and references therein). Up to 35 states have been used during these calculations in order to reach an excited state significantly coupled with the ground state.

II. Discussion and Outlook

A. Choice of a Theoretical Approach. In 2003, Jaska et al. published the X-ray structures of several aminoborane dimers (see Figure 2 of the present work or Figures 1−3 in ref 12). First we have selected the smallest system (structure **I** of Figure 2) in order to check the necessary level of approximation needed to obtain converged theoretical results. The corresponding results are given as Supporting Information. Note that **I** presents the D_{2h} symmetry in our gas-phase calculations.[40] We found the following:

1. Most of the methods provide similar valence angles: the largest variations are 1° for α_{B-N-B}.

2. For bond lengths, the MP2 and MP4(SDQ) approaches give similar values (∼0.002 Å). Therefore, one can assume that MP2 provides *theoretically converged* bond lengths.

3. The N−C distance is estimated to be very close to 1.47(5) Å, but for HF and PBE0 (1.46 Å).

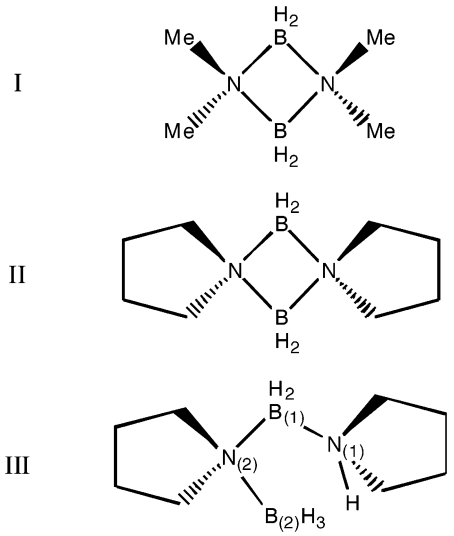

Figure 2. Representation of the three structures studied in Table 1.

4. The B−N bond lengths are more contrasted. The longest (shortest) bonds are obtained for B3LYP (PBE0), whereas the MP2 and MP4(SDQ) distances stand in between.

5. The addition of diffuse or polarization functions on the hydrogen atoms has no impact on the geometries. On the other hand, two sets of *d* functions centered on N and B are required to attain basis set saturation.

6. At the HF and DFT levels, 6-31G(2d) provides converged geometrical bond lengths. Actually, the variations observed when adding extra sets of polarization functions or when using triple-ζ basis sets are very small. For instance, the maximum differences in N−C and B−N bond lengths when going from 6-31G(2d) to 6-311+G(2df,p) are 0.001 Å.

7. At the MP2 and MP4(SDQ) levels, a triple-ζ basis [6-311G(2d)] is necessary to reach converged values. From a purely methodological point of view, we have, at this stage, retained the HF/6-31G(2d), DFT[B3LYP, B98 and PBE0]/6-31G(2d), and MP2/6-311G(2d) approaches because they yield bond distances that are converged with respect to the basis set

TABLE 2: Relative Energy per Unit Cell for the Four Conformers (TC Energy Is Set to Zero by Convention) of the Hexamer ($N = 6$)[a]

method	TC	TT	HEL	COIL
HF/6-31G(2d)//HF/6-31G(2d)	0.00	+4.96	−0.96	+0.12
PBE0/6-31G(2d)//PBE0/6-31G(2d)	0.00	+6.23	−0.94	−0.66
MP2/6-311G(2d)//PBE0/6-31G(2d)	0.00	+5.61	−1.17	−0.84
MP2/6-311++G(2d,p)//PBE0/6-31G(2d)	0.00	+5.59	−1.14	−0.97
MP2/6-311G(2d)//MP2/6-311G(2d)	0.00	+5.62	−0.96	−1.32
MP2/6-311++G(2d,p)//MP2/6-311G(2d)	0.00	+5.59	−0.83	−1.46

[a] All values are given in kcal/mol. TC, TT, HEL, and COIL acronyms are defined in section II.B and Figure 3.

size. The fact that the more elaborated approach (MP2) requires a larger basis set to reach its full potential is not surprising.

In Table 1, the experimental and theoretical structures of **I**, **II**, and **III** are compared. In the (actual) triclinic crystal, the D_{2h} symmetry of **I** is lost. For **I**, the d_{B-N} values are too long at the HF, B3LYP, and B98 levels, whereas the MP2 values are slightly overestimated and the PBE0 d_{B-N} values are closer to the experimental range. Note that in the weakly bonded[41] borazane (BH_3NH_3), d_{B-N} is strongly shortened[42] when going from gas-phase to solid state. Such a solid-state effect may affect structure **I**, but it is probably less significant. On the contrary, for d_{N-C}, we found a nice experimental/theoretical agreement for B3LYP/B98 whereas the MP2 d_{N-C} distances are a bit too small and HF/PBE0 underestimate the values. The agreement between the X-ray and the theoretical α_{B-N-B} and α_{N-B-N} is excellent, especially with the PBE0 functional. On the other hand, the theoretical α_{C-N-C} and α_{B-N-C} angles are systematically too blunt and too sharp, respectively. It can consequently be concluded that HF quite poorly describes bond lengths, B3LYP (PBE0) provides reliable external methyl-substituent (BN core) structural parameters, and MP2 gives an advantageous compromise with limited deviations for each distance. As the crystal packing effects are probably stronger on the periphery of the molecule, one can state that PBE0 is hic et nunc the most interesting approach. More importantly, the poor description of the methyl group by PBE0 has no effect on our calculations, as the actually synthesized PAB[3−5] studied in the following does not present any N−C bonds (but in ref 1). The trends found for **II** are similar (Table 1), with the best theory/experiment agreement obtained with PBE0/6-31G(2d). On top of that, the PBE0/6-31G(2d) N−C distance is in line with the experimental value. For structure **III** (Table 1), the central NB bond is shorter than the terminal bonds. All ab initio approaches reproduce this feature but the terminal bond lengths are systematically too long, especially at the HF level. The closest estimate is, once again, obtained with PBE0 although the overestimation remains substantial. This theory/experiment discrepancy is probably due to the fact that, in the experiment,[12] hydrogen bonds show up and **III** tends to dimerize.

For all these reasons, our methodological ace for evaluating the aminoborane geometries is PBE0/6-31G(2d), since it provides the best theory/experiment agreement for the backbone geometrical data. Except when noted, PBE0/6-31G(2d) will be the default level of approximation used for all the geometry/vibration calculations described in the following. Nevertheless, we keep in mind that MP2/6-311G(2d) leads to *theoretically converged* geometries.

For the other properties we study in this article (relative energies, charges, excitation spectra, etc.), no experimental data are available. Consequently, we have tried to obtain the best predictive theoretical evaluation possible. The results are given in Tables 2−4. For the energy, HF (PBE0) underestimates

TABLE 3: MK Charges (in *e*) on the Central Atoms of the TC PAB Tetramer ($N = 4$, PBE0/6-31G(2d) Geometry)

method	N	B	method	N	B
HF/6-31G(2d)	0.38	−0.28	MP2/6-311++G(2d)	0.31	−0.24
HF/6-311G(2d)	0.26	−0.16	MP2/cc-pVTZ	0.30	−0.20
MP2/6-31G(2d)	0.46	−0.39	HF/6-311G(2d)[a]	0.28	−0.16
MP2/6-311G(2d)	0.32	−0.25	MP2/6-311G(2d)[a]	0.36	−0.24
MP2/6-311G(3df)	0.36	−0.29			

[a] On the MP2/6-311G(2d) geometry.

TABLE 4: Singlet-State Excitation Energies in eV[a]

	method		
basis	TD-PBE0	TD-B3LYP	CIS
6-31G(2d)	7.7	7.4	10.2
6-311G(2d)	7.0	6.7	9.2
6-31+G(2d)	6.3	6.0	8.2
6-311+G(2d)	6.3	6.1	8.2
6-311++G(3d,p)	6.2	5.9	8.1
cc-pVDZ	7.2	6.9	9.6
aug-cc-pVDZ	6.2	5.9	8.0
d-aug-cc-pVDZ	6.1	5.9	
6-311+G(2d)[b]	6.3	6.0	8.2

[a] The reported values correspond to the first excited state and have been obtained on the dimer ($N = 2$) in the TC conformation [PBE0/6-31G(2d) geometry]. [b] On the MP2/6-311G(2d) geometry.

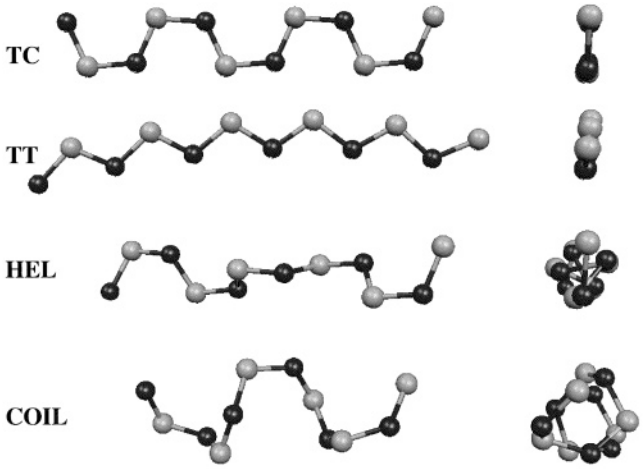

Figure 3. Side (left) and top (right) views of the PBE0/6-31G(2d) optimized structures of the six central cells of the PAB dodecamer ($N = 12$). From top to bottom: TC, TT, HEL, and COIL conformations. Nitrogen atoms are in dark gray, and boron nuclei in light gray; hydrogen atoms have been omitted for clarity.

(overshoots) the difference between trans−cisoid (TC) and trans−transoid (TT) conformations (see Figure 3 and section II.B for a description of these conformations). The addition of diffuse functions does not significantly modify the results. MP2 and PBE0 geometries provide the same relative stability for TC/TT, but the ordering of the helicoidal (HEL)/coiled (COIL) conformers is inverted. However, the relative stability of the nonplanar PAB oligomers remains in the same range (around −1 kcal/mol per cell) for all geometries. It appears that the Mulliken scheme yields unreliable partial atomic charges. Indeed, no consistency with respect to basis set extension could be found. In the MK framework, the MP2/6-311G(2d) charges are in good agreement with those obtained with larger basis sets (such as cc-pVTZ) and the addition of diffuse functions (or extra polarizations) only leads to small variations of q^N and q^B. As a consequence, the MP2/6-311G(2d)//PBE0/6-31G(2d) approach has been selected for the estimation of both the relative energies and the partial atomic charges. For the vertical

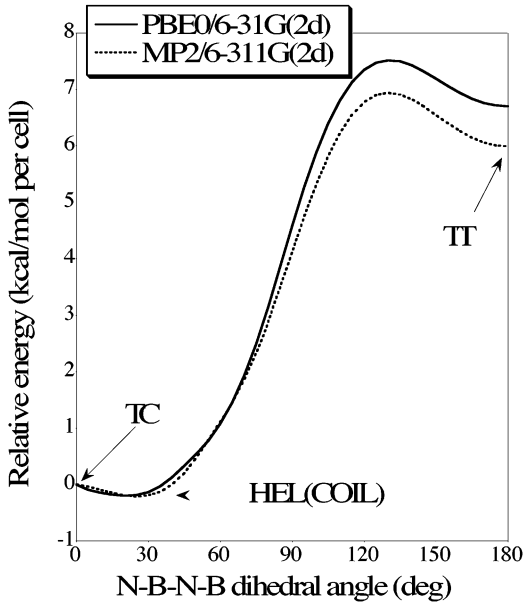

Figure 4. PBE0/6-31G(2d) and MP2/6-311G(2d) rotational profiles (kcal/mol per cell) for the PAB dimer ($N = 2$ in Figure 1). The same method is used to compute the energy and to optimize the geometries. TC, HEL(COIL), and TT labels indicate the positions of the trans−cisoid, helicoidal (coiled), and trans−transoid conformations. By convention, the relative energy of the former has been set to zero. These profiles are symmetric with respect to $\tau_{N-B-N-B} = 180°$.

excitation energies (Table 4), CIS values are too large as foreseen. B3LYP and PBE0 are in good agreement with slightly smaller excitation energies for the former. This is consistent with the smaller amount of exact (HF) exchange included in B3LYP (20%) [PBE0 (25%)]. The use of diffuse functions appears mandatory to avoid a 1 eV overestimation of the excitation energies, whereas extra polarization functions are unnecessary, as already stated for the other properties. These conclusions are in good agreement with previous studies of small organic systems.[43] The use of two sets of diffuse functions (*d-aug*-cc-pVDZ) does not modify the excitation energies. As a result, the TDDFT/6-31+G(2d)//PBE0/6-31G(2d) approach has been chosen for the evaluation of vertical excitation energies.

B. Conformations and Relative Energies. The rotational profile (around the N−B−N−B dihedral angle) of the PAB dimer is shown in Figure 4. The shapes obtained at the PBE0/6-31G(2d) and MP2/6-311G(2d) levels are very similar. Consistent with Table 2, the only significant difference is the relative stability of the TT chains. Among the planar conformations, the TC chains are more stable than the TT oligomers. Moreover, a 25.5° [44] deviation of the dihedral angle in the TC dimer leads to the global minimum, identified as the HEL [or COIL, see below] conformation. Although less energetically favored, the TT compound corresponds to a minimum in the rotational profile whereas the TC chain is similar to a transition state (TS) between two helicoidal structures (one with a positive dihedral angle, one with a negative dihedral angle). This is confirmed by a vibrational analysis: all the frequencies of the TT dimer are real, whereas its TC counterpart presents one imaginary frequency. The NBNB rotation barrier (7 kcal/mol per cell) displayed in Figure 4 is relatively small: it is easy to modify the conformation of PAB. For comparison purposes, in polyphosphazene (PP), which is considered to be very flexible, the rotation barrier between TT and TC is 5 kcal/mol per cell.[45] For the phosphorus-parent to PAB, polyphosphinoborane (PPB), the calculated rotational profile has a similar shape and the height of the rotation barrier is only half of the one found for PAB.[46] The small PAB rotation barrier is consistent with the backbiting phenomena found by Jaska and co-workers.[12] However, if flexibility was the only parameter, the backbiting would also occur during the synthesis of PPB on the same rhodium catalyst. As that is not the case, this suggests that extra parameters are playing a major role. Indeed, we note that (i) the substituents in the experimental PAB of ref 12 (Me, or 1,4-C_4H_8) differ from those of PPB (^{i}Bu, Ph, etc.)[47,48] and (ii) the geometries of the two macromolecules significantly differ, with B−N (B−P) distances around 1.6 (1.9 Å). The same statement holds for the partial atomic charges. This indicates that the type of polymerization reaction is different for PAB and PPB, consistent with measurements.[15]

TABLE 5: Relative Energy per Unit Cell for the Four Conformers (TC Energy Is Set to Zero by Convention)[a]

N	TC	TT	HEL	COIL
2	0.00 [0.00]	+5.95 [+5.67]	−0.13 [−0.06]	−0.13 [−0.06]
4	0.00 [0.00]	+6.00 [+5.70]	−1.10 [−1.04]	−1.01 [−0.86]
6	0.00 [0.00]	+5.61 [+5.32]	−1.17 [−1.10]	−0.84 [−0.70]
8	0.00 [0.00]	+5.27 [+4.98]	−1.21 [−1.14]	−0.75 [−0.60]
10	0.00 [0.00]	+5.09 [+5.05]	−1.25 [−1.19]	−0.71 [−0.59]
12	0.00	+4.93	−1.28	−0.70

[a] All values have been obtained with the MP2/6-311G(2d)//PBE0/6-31G(2d) approach and are given in kcal/mol. *N* is the number of unit cells. For the dimer, HEL and COIL chains are the same. Between brackets are the relative energies corrected by using the PBE0/6-31G(2d) ZPVE amplitude.

For longer chains, there are numerous possible dihedral angles for the PAB backbone. To identify the most stable structures, two procedures have been followed:

1. We distort the TC tetramer ($N = 4$) geometry, along the three vibrational coordinates presenting imaginary frequencies. The resulting geometries are used as starting points for geometry optimizations, leading to two hypothetical structures.[49] Note that, for one of the two structures, one chain end tends to form a coiled structure rather than an helix.[50] This point is studied in the following section.

2. A cautious analysis of the results of procedure 1 shows that the variations of the dihedral angles with respect to the planar TC form are always ±30° for dihedral N−B−N−B angles and ±10° for B−N−B−N dihedral angles (neglecting the terminal coil). If helicoidal chains present a periodic structure, there are six nonequivalent possibilities remaining (for the polymer).[51] We have used these six geometries as starting points for additional geometry optimizations.

Some of the stationary geometries determined by this second procedure are equivalent to those obtained via procedure 1. From procedures 1 and 2, it turns out that the most stable helicoidal tetramer presents a terminal coil with successive dihedral angles, from the NH_3 end to the BH_3 end, of 29.7, 166.7, 54.6, −124.0, and 38.8°. This structure corresponds to an energetic well as confirmed by analysis of vibrational spectra (no imaginary frequency). Optimizations carried out on longer chains show that the coil is always limited to the last two cells, and therefore this phenomena has to be classified as a purely chain-end effect. The spatial extension of the TT, TC, and HEL systems mainly takes place in one direction (see Figure 3). However, as noted for PP[45] and for PPB[46] and as observed on the last few cells of the helix, flexible inorganic polymers can form coiled structures. We have tested this possibility, and it appears that (at least) one coil presents a stability similar to that of the helix.[52]

Table 5 gives the relative energies of increasingly long PAB oligomers in the four considered conformations (Figure 3). As could be expected for conformers of a given compound, the

TABLE 6: Bond Lengths of PAB Oligomers Measured at the Chain Center[a]

	Planar							
	TC				TT			
N	d_{B-N}	d_{N-B}	d_{N-H}	d_{B-H}	d_{B-N}	d_{N-B}	d_{N-H}	d_{B-H}
2	1.569	1.605	1.016	1.212	1.533	1.652	1.017	1.207
4	1.567	1.587	1.019	1.222	1.562	1.629	1.020	1.206
6	1.580	1.584	1.018	1.219	1.575	1.612	1.020	1.206
8	1.584	1.581	1.018	1.219	1.582	1.604	1.020	1.206
10	1.587	1.579	1.018	1.218	1.586	1.600	1.020	1.206
12	1.589	1.578	1.018	1.218	1.588	1.598	1.020	1.205
14	1.590	1.577	1.017	1.218	1.590	1.597	1.020	1.205
16	1.591	1.577	1.017	1.218	1.590	1.596	1.020	1.205
	Nonplanar							
	HEL				COIL			
N	d_{B-N}	d_{N-B}	d_{N-H}	d_{B-H}	d_{B-N}	d_{N-B}	d_{N-H}	d_{B-H}
2	1.568	1.604	1.016	1.211	1.568	1.604	1.016	1.211
4	1.563	1.578	1.016	1.221	1.575	1.595	1.018	1.214
6	1.565	1.585	1.020	1.218	1.579	1.576	1.018	1.212
8	1.572	1.578	1.019	1.218	1.565	1.596	1.018	1.216
10	1.574	1.577	1.019	1.218	1.587	1.580	1.019	1.215
12	1.577	1.575	1.019	1.217	1.569	1.591	1.018	1.216
14	1.578	1.574	1.019	1.217				
16	1.579	1.574	1.019	1.217				

[a] d_{B-N} is the length found of the central bond (even numbered), whereas d_{N-B} is the length of the previous bond (odd numbered). All values are in Å and have been obtained at the PBE0/6-31G(2d) level. For HEL and COIL, the reported N−H and B−H distances correspond to the shortest bonds at the center of the oligomers.

zero-point vibrational energy (ZPVE) corrections have almost no impact on the relative stabilities. When chains get longer, the energetic difference between TC and TT/COIL decreases whereas HEL chains become more and more stabilized. For long chains, the relative energies stabilize, and we can estimate the polymeric values to be close to 0.0 (TC), +4.0 (TT), −1.3 (HEL), and −0.6 (COIL) (kcal/mol per cell). These differences are small. Therefore, for the macromolecule, the two off-planar conformers are predicted to be almost energetically equivalent and only slightly preferred to the TT structure. As a consequence, it is reasonable to think that the four conformations of PAB might coexist. At least, the results of Table 5 do not allow one particular conformation to be disregarded as being too unstable. Although showing vibrational modes with imaginary frequencies, TC conformers might be favored by a substitution of PAB by side groups or by special experimental conditions (quick-cooling).

C. Geometries. The bond lengths and valence angles of the four PAB conformers are reported in Tables 6 and 7, respectively. Table 8 summarizes the central dihedral angles of the HEL and COIL chains.

Except for the COIL, it appears that the bond lengths become almost constant for the longest chains. However, as seen in Figure 3, the asymmetric (repeating) unit cell in COIL contains more backbone atoms (eight) than the other structures. Therefore, the results of Tables 6 and 7 are composed of two series for the COIL: one for $N = 6, 10, ...$ and another for $N = 8, 12, ...$ In Table 6, the most striking feature is the nonzero amplitude of the bond length alternation (BLA) in the TC structure whereas, for sufficiently long chains, all bonds seem to become equivalent in TT, consistent with previous evaluations.[16] For HEL, we predict a slightly alternant pattern for the polymer.[53] In the asymmetric unit cell of COIL, at least one bond is always shorter than the three others. Therefore PAB parallels PPB with alternating TC, slightly alternating HEL, and

TABLE 7: Selected PBE0/6-31G(2d) Central Valence Angles (in Degrees) of PAB Oligomers

	Planar							
	TC				TT			
N	α_{B-N-B}	α_{N-B-N}	α_{H-N-H}	α_{H-B-H}	α_{B-N-B}	α_{N-B-N}	α_{H-N-H}	α_{H-B-H}
2	118.0	106.3	104.9	113.8	113.7	108.6	106.3	115.8
4	119.1	110.1	102.1	111.8	113.8	108.3	107.1	115.6
6	118.7	109.7	103.3	112.3	113.7	108.3	106.0	115.5
8	118.8	110.0	103.3	112.3	113.6	108.3	106.1	115.5
10	118.7	110.0	103.5	112.4	113.5	108.4	106.1	115.5
12	118.8	110.1	103.5	112.4	113.4	108.3	106.1	115.5
14	118.8	110.1	103.6	112.4	113.3	108.4	106.1	115.5
16	118.8	110.2	103.6	112.5	113.4	108.3	106.1	115.5
	Nonplanar							
	HEL				COIL			
N	α_{B-N-B}	α_{N-B-N}	α_{H-N-H}	α_{H-B-H}	α_{B-N-B}	α_{N-B-N}	α_{H-N-H}	α_{H-B-H}
2	117.1	105.8	104.5	114.1	117.1	105.8	104.5	114.1
4	118.4	108.3	105.7	111.8	124.9	109.5	104.5	111.0
6	116.2	108.6	102.6	112.7	124.9	110.8	104.6	108.1
8	116.1	108.8	103.6	112.6	122.2	112.0	103.7	110.8
10	116.4	109.0	103.5	112.7	125.6	110.3	104.4	110.3
12	116.3	109.0	103.7	112.8	122.7	112.1	103.8	110.7
14	116.3	109.1	103.7	112.8				
16	116.3	109.1	103.7	112.9				

TABLE 8: Central Dihedral Angles of PAB Oligomers[a]

	HEL		COIL			
N	$\tau_{N-B-N-B}$	$\tau_{B-N-B-N}$	$\tau_{N-B-N-B}$	$\tau_{B-N-B-N}$	$\tau_{N-B-N-B}$	$\tau_{B-N-B-N}$
2	20.6				20.6	
4	54.6	166.7		−90.3	53.6	−83.1
6	38.0	170.9	49.0	−80.2	−25.0	−87.0
8	39.3	172.9	−26.0	−84.4	50.7	−86.6
10	41.4	170.8	50.8	−85.6	−21.1	−85.2
12	40.6	172.3	−22.1	−84.8	50.9	−84.5
14	41.5	171.6				
16	41.9	172.0				

[a] All values are given in degrees and have been obtained at the PBE0/6-31G(2d) level.

nonalternating TT patterns,[46] although saturation with respect to the oligomer length is reached for much shorter chains in PPB. Experimental XPS spectra[10] indicate that there is only one type of BN bond in PAB. If this experimental result does not rule out oligomers with slightly different BN bond lengths, it might also be explained by the synthesis of cyclic rather than extended structures. Long TC and HEL structures present long bonds (the central B−N bonds, parallel to the longitudinal axis of PAB) and short bonds (the N−B bonds, perpendicular to the longitudinal axis). Consistent with experiment,[11,12] the reverse is found for the short chains, with the longest bonds at the extremities. According to a natural bond order (NBO) analysis,[54] these shorter bonds are purely single bonds and do not exhibit any significant double bond character. For the polymer, the estimated BLA of TC is 0.016 Å ± 0.002 Å. Such a BLA is similar to that of TC-PPB[46] (0.018 Å) or TC-PP[45] (0.024 Å) but much smaller than in TT-polyacetylene[55] (0.062 Å). The N−H and B−H bond lengths do not significantly depend on the oligomer length or on the conformation, the only exception being slightly shorter B−H bonds in the TT compounds. The computed bond lengths (N−H = 1.02 Å and B−H = 1.21−1.22 Å) are in perfect agreement with normalized values given in the literature (N−H = 1.03 Å and B−H = 1.21 Å).[56] For TT, the geometries we determined are also in good agreement with previous periodic MP2/6-31G(d,p) calculations:[16] $d_{B-N} = d_{N-B} = 1.601$ Å, $d_{B-H} = 1.199$ Å, and $d_{N-H} = 1.019$ Å.

TABLE 9: Polymeric Theoretical and Experimental Vibrational Circular Frequencies of Polyaminoborane[a]

	theory[b]			experiment				
bands	TT	HEL	COIL	ref 5[c]	ref 4[d]	ref 3[e]	ref 1[f]	ref 9
N−H str	3410	3380	3350	3330	3300	3280	3276	3320−3220
N−H str	3320	3230	3250	3280				
B−H str	2530	2400	2380	2360	2340	2380	2400	2380−2280
B−H str	2480						2305	
B−H str	2410							
N−H def	1610	1620	1610	1550	1600	1560	1595	1575
	1380	1370	1380	1400	1380	1380	1380	1405
		1200	1210	1200	1160	1180	1236	
							1173	
	1110		1090		1040	1090		
						1060		
	930	880		860	850	840		

[a] All values are in cm^{-1}. [b] This work. The values have been obtained from PBE0/6-31G(2d) calculations (scaling factor, 0.97; fwhm = 50 cm^{-1}) on oligomers $N = 6$, 8, and 10, followed by an extrapolation to $N = \infty$. [c] The peaks have been estimated from the spectra reproduction given in ref 5. Values given by the authors in the text: 3300, 2350, 1560, and 1400 cm^{-1}. [d] Shoulders and some very weak peaks have been neglected. [e] Peaks estimated in ref 4 from spectra reproduction of ref 3. [f] For poly(methylaminoborane). Some weak peaks and the typical methyl bands have been neglected.

The valence angles also converge rapidly with the chain length. Indeed, it is found that the largest variations between $N = 10$ and $N = 12$ are 0.1° only (except for COIL, due to the four-cell periodicity). For all the conformations, the B−N−B angle is larger (by at least 5°) than the N−B−N angle. Note that the reverse has been determined and is confirmed by experience[12] for the four-member rings **I** and **II**, whereas for structure **III** the difference is much smaller (1°), indicating that the formation of rings and the presence of side substituents strongly affect the backbone angles. The largest differences between conformers arise for B−N−B. Indeed, the α_{B-N-B} ordering is COIL (123 and 126°) > TC (119°) > HEL (116°) > TT (113°). The H−N−H angles are always smaller than the H−B−H angles by ∼10°, and the variation is small when going from one conformation to the other. Qualitatively, the same type of behavior was found in PPB.[46]

The central dihedral angles (Table 8) of the HEL chains become almost constant provided $N \geq 6$. Therefore, we can estimate the polymeric angles to be close to 40 and 171° for $\tau_{N-B-N-B}$ and $\tau_{B-N-B-N}$, respectively. For COIL, the four-cell pattern appears clearly. For the polymer, the $\tau_{B-N-B-N}$ is always around −85° whereas the $\tau_{N-B-N-B}$ is alternatively close to −22° and +51°.

D. Vibrational Analysis. In Table 9, a comparison between the computed IR spectra of TT, HEL, and COIL and the available experimental values is carried out. Obviously, the worst agreement with experimental values is observed for the TT chains. This is particularly striking for the B−H stretching mode for which a peak at 2530 cm^{-1} lies higher than any experimentally observed B−H stretching band. The agreement between experimental and theoretical values for the N−H stretch in TT chains is poor as well. Therefore, the results of Table 9 indicate that the experimentally synthesized PAB probably takes the HEL or the COIL conformation. This assessment is consistent with their greater stability. For both conformers, the agreement between theoretical and experimental spectra is excellent, the largest deviations being of the same amplitude as the discrepancies between the experimental values. Compared to the older measurements, the N−H stretch frequency looks a bit overestimated, but it is in good agreement with the latest measurements.[5] By comparison to the results obtained on polyborazine (1450 cm^{-1}), the 1380 cm^{-1} peak was labeled as the signature of the BN stretch by Kim and co-workers.[5] However, in our calculations, this peak corresponds to a vibration of the terminal NH_3 (umbrella-like mode) with a relative intensity decreasing with increasing oligomer size. Our findings are consistent with other theoretical and experimental findings. Indeed, in borazane this umbrella mode has a circular frequency of 1343 cm^{-1} [41,57,58] and this frequency is higher in the solid state.[42] Consistent with the 1450 cm^{-1} result obtained on polyborazine, we have evaluated the BN stretch to be 1468 cm^{-1} in borazine.[59] For aminoborane (BH_2-NH_2), this stretch is moved toward smaller energies: the experimental value[60] is 1337 cm^{-1}, in perfect agreement with our[59] 1343 cm^{-1} or with other previous theoretical investigations.[61] However, the strength of the BN bonds in aminoborane or borazine is expected to be larger than in PAB. Indeed, for borazane, the BN stretch is around 968 cm^{-1} (experimental[58] value) and presents a significant anharmonic component (harmonic frequency, 662 cm^{-1})[41] due to the strong van der Waals character of the BN bond in that system.[41] In PAB, one expects the BN stretch to be between the results of borazane and aminoborane: this is what we observed with harmonic stretches around 900 cm^{-1}. Consistently, the assignment of the 1380 cm^{-1} peak to be a BN stretch is not supported by our results, as this peak appears to be related to the presence of terminal NH_3. As the dipole moment variation occurring during the umbrella mode is very large and as this peak presents a frequency different from other PAB vibrations, it is likely that one would notice this peak even if the quantity of terminal NH_3 is relatively small. This could indicate either that the polymerization is not complete or that some solvent or monomeric units are left inside the polymer. For cycloborazane, this peak is not present in our theoretical simulations. In the experiment, the situation is less clear with results depending on the size of the ring.[62]

To provide a more complete vibrational description of the COIL, HEL, and TT, we have reproduced the IR spectra in Figures 5 and 6. For the decamer, the frequencies of the peaks in the 800−1600 cm^{-1} region are close to convergence with respect to N (Figure 5). The differences between COIL/HEL and TT are substantial: TT presents a strong peak around 1100 cm^{-1}, whereas HEL and COIL display absorption in a much broader range (1100−1200 cm^{-1} region). Nevertheless, the COIL spectrum is more flat than its HEL counterpart and it is difficult to distinguish them even with a 25 cm^{-1} resolution. For the B−H stretching region (Figure 6), one should be more cautious because (1) the values for the decamer are further away from convergence and (2) solid-state effects are stronger as suggested by the N−H/B−H interaction pattern (see the next section). However, it is clear that TT chains show a vibrational spectrum shifted toward higher frequencies with the strongest absorption at 2550 cm^{-1}. Overall, HEL and COIL have similar spectra with a 25 cm^{-1} resolution, the only significant difference being, once again, the slightly larger peaks for COIL and the displacement of the higher-frequency peak from 2470 cm^{-1} (COIL) toward 2490 cm^{-1} (HEL).

E. Charges and Dipole Moments. Table 10 summarizes the charge borne by the central atoms and the norm of the dipole moment for increasingly long PAB chains. For $N = 8$ or 10, the charges are mostly converged and are quite similar for the four conformations with the notable exception of TC chains for which a sign inversion between N and B is observed. For the other conformers, the charge separation between N and B is decreasing with the increase of stability of PAB, that is, $\Delta q = q^B - q^N$ follows TT > COIL > HEL, whereas the charge

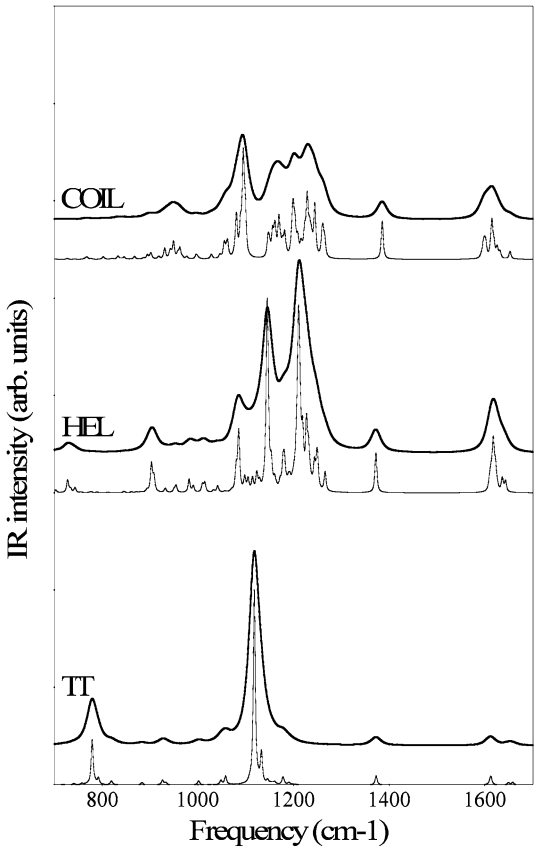

Figure 5. IR spectra: 600−1200 cm^{-1} region for three conformations of the decamer. These results have been obtained at the PBE0/6-31G(2d) level. Frequencies have been scaled by a factor of 0.97. Two resolutions are presented: 5 cm^{-1} (thin line) and 25 cm^{-1} (thick line).

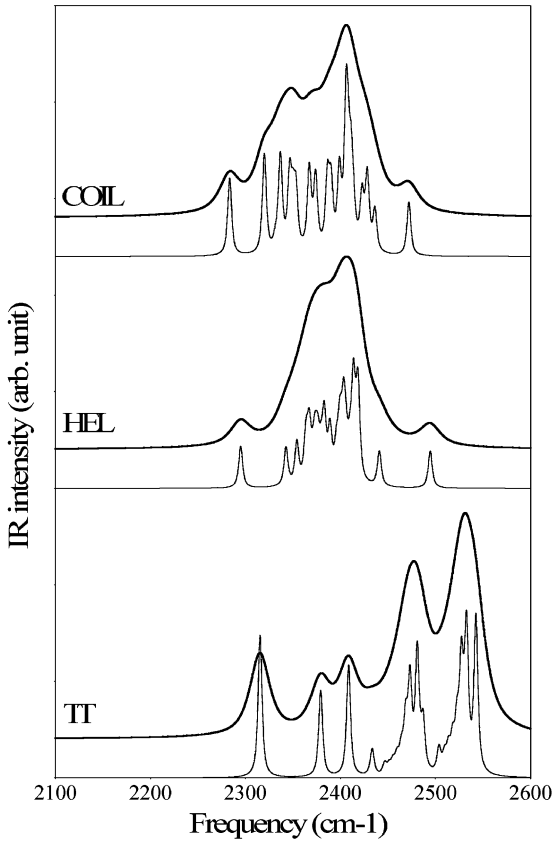

Figure 6. Offset of the decamer IR spectra (three conformations): the B−H stretching region. See Figure 5 for more details.

borne by the hydrogen atoms is always close to 0.2 *e* for H(N) and −0.2 *e* for H(B). These results are completely consistent with the weak attractive intermolecular interaction suggested by Jaska[12,63] with the $N-H^{\delta+}\cdots^{\delta-}H-B$ pattern. The reversal of the sign in the TC chain is probably related to its TS-like structure. Using the CHELPG scheme, the same charge inversion is found when going from TT (HEL or COIL) to TC. For the tetramer, we have identified the TS (one imaginary frequency) that relates the hypothetical TC to the stable COIL. For this system, it turns out that $q^N = -0.16$ *e*, $q^B = -0.02$ *e*, and $\Delta q = 0.14$ *e*, suggesting that the sign inversion is only present in systems presenting more than one imaginary frequency. Note that the charge separation in PAB is smaller than in PPB[46] for which $q^P = 0.4$ *e* and $q^B = -0.2$ *e*, although the electronegativity difference between P and B is much smaller than between N and B.

The dipole moment per unit cell, $|\Delta\mu(N)| = (1/2)|\mu(N)| - (1/2)|\mu(N-2)|$, is almost constant with chain length but is not fully smooth.[64] Nevertheless, we can predict polymeric values ($|\Delta\mu(\infty)|$) of 2.5 D (TC and HEL), 4 D (TT),[65] and 2 D (COIL) for the different conformers. These differences are large enough to allow the discrimination of TT from TC, HEL, and COIL. One can rationalize this ranking by saying that each N−B bond brings a small contribution to $|\mu|$. Indeed, the bonds in coiled chains are pointing in distributed directions leading to a significant averaging of "bond dipole moments" and a weak total value, whereas TT chains have a perfect order of the bonds, giving a large total norm. For comparison, TC PP has a $|\Delta\mu(8)|$ of 7 D[66] whereas the corresponding PPB values are $|\Delta\mu(\infty)|$ of 3 (7) D for COIL (TT), as a result of a stronger charge separation in PP and PPB.

TABLE 10: MP2/6-311G(2d) Norm of the Dipole Moment (Debye) and MK Charges of the Central Atoms of PAB Oligomers (in *e*, PBE0/6-31G(2d) Geometries)[a]

Planar

	TC					TT				
N	$\|\mu\|$	N	B	H(N)	H(B)	$\|\mu\|$	N	B	H(N)	H(B)
2	4.03	−0.10	0.21	0.18	−0.20	10.96	−0.34	0.42	0.23	−0.20
4	9.28	0.32	−0.25	0.13	−0.13	23.19	−0.30	0.15	0.18	−0.13
6	15.15	0.30	−0.28	0.12	−0.12	35.89	−0.46	0.35	0.23	−0.18
8	21.25	0.37	−0.36	0.11	−0.11	48.60	−0.26	0.28	0.18	−0.17
10	27.45	0.36	−0.36	0.12	−0.12	61.00	−0.41	0.31	0.21	−0.17
12	33.74	0.39	−0.37	0.11	−0.12	72.96	−0.34	0.31	0.19	−0.17
14	40.00	0.40	−0.38	0.11	−0.12	84.56	−0.37	0.31	0.20	−0.17

Nonplanar

	HEL					COIL				
N	$\|\mu\|$	N	B	H(N)	H(B)	$\|\mu\|$	N	B	H(N)	H(B)
2	4.22	−0.20	0.23	0.21	−0.21	4.22	−0.20	0.23	0.21	−0.21
4	7.39	−0.22	0.14	0.24	−0.20	6.99	−0.20	0.16	0.24	−0.21
6	11.66	−0.14	0.16	0.22	−0.22	9.59	−0.22	0.20	0.25	−0.21
8	17.04	−0.18	0.18	0.22	−0.23	14.35	−0.33	0.14	0.28	−0.20
10	23.54	−0.10	0.13	0.21	−0.22	19.39	−0.12	0.23	0.21	−0.25
12	30.35	−0.05	0.15	0.19	−0.22	24.06	−0.16	0.26	0.22	−0.24
14	36.88	−0.08	0.10	0.21	−0.21					

[a] For nonplanar chains, the reported figures are given for the hydrogen bearing the largest charge.

F. Excitation Energies. The vertical excitation energies of PAB are given in Table 11. For the hexamer and the octamer, the first excited state (FES) lies ∼5 eV above the ground state, except for the TT chains for which the excitation energy is 3 eV. The energy of the FES is not yet converged at this chain

TABLE 11: Singlet-State Excitation Energies in eV[a]

	PBE0				B3LYP			
N	TC	TT	HEL	COIL	TC	TT	HEL	COIL
				FES				
2	6.3	4.8	6.3	6.3	6.0	4.5	6.0	6.0
4	5.7	3.7	6.0	6.2	5.3	3.3	5.6	5.9
6	5.4	3.2	5.7	6.0	5.0	2.8	5.2	5.6
8	5.3	3.0[b]	5.5	5.7	4.8	2.5[b]	5.0	5.3
				FCES				
2	6.3	6.0	6.3	6.3	6.0	5.7	6.0	6.0
4	6.3	6.3	6.5	6.8	6.0	6.0	6.3	6.5
6	6.2	6.3	6.4	6.8	6.1	5.9	6.2	6.5
8	6.2		6.4	6.8	6.0		6.2	6.5

[a] These values have been obtained with the B3LYP/6-31+G(2d) and PBE0/6-31+G(2d) schemes on the PBE0/6-31G(2d) geometries. The reported values are the first excited state (FES) and the first excited state that couples [oscillator strength > 0.01] with the ground state (FCES). [b] For the TT octamer, the use of 6-31+G(2d) leads to quasi-linear dependencies, i.e., some of the eigenvalues of the metric matrix are smaller than 10^{-6}. Consequently, some of the basis set dimensions were removed for these calculations.

length. At this stage, it is difficult to estimate an asymptotic polymeric value. For the states that couple with the ground state (FCES), a rapid convergence is obtained (FCES amplitudes are almost constant for $N = 4$, 6, and 8). The deviations of the conformers' FCES are quite small with only 0.5 eV between TT and COIL. The smaller excitation energies in the TT chains can be related to their planarity and to the absence of BLA. As for PPB [B3LYP/6-311G(d)], the FCES is 6 eV above the ground state,[46] a large value if compared to that of conjugated systems but small when compared to that of the isoelectronic polyethylene.[67,68]

The ionization potentials (electroaffinities) computed for PAB at the OVGF[69]/6-311+G(2d) level are 10.1, 10.1, and 9.5 eV (−0.8, −0.8, and −1.0 eV) for the TC, HEL(COIL), and TT dimers, respectively. This corresponds to a Mulliken electronegativity (hardness) of 4.7 (5.5), 4.7 (5.5), and 4.3 (5.3) eV, respectively.

III. Conclusions

We have studied the structures and the properties of long PAB oligomers. It turns out that PAB is flexible: a complete rotation around the BN backbone only requires 7 kcal/mol per cell. Four conformations have been investigated: trans−cisoid, trans−transoid, helical, and coiled. It appeared that TC chains are unstable transition-state-like structures that would not be obtained experimentally, except in peculiar conditions. The analysis of the IR spectra demonstrates that the synthesized PAB cannot be associated with the less stable TT conformation. This TT chain differs from the other conformers in many aspects: it presents a zero bond length alternation, has a larger dipole moment, and shows smaller vertical excitation energies. Finally, with regard to the experimental vibrational data, both the HEL and COIL compounds (which have similar stability, dipole moments, partial atomic charges, excitation energies, etc.) could correspond to the experimental PAB. The presence of an experimental IR peak around 1380 cm^{-1} seems to indicate the presence of (a substantial) terminal NH_3 in the reaction. This could mean that the molecular weight of the synthesized PAB might be quite small.

Acknowledgment. D.J. and E.A.P. thank the Belgian National Fund for their research associate positions. We acknowledge the support from the Interuniversity Attraction Poles Programme on "Supramolecular Chemistry and Supramolecular Catalysis (IUAP No. P5-03)" from the Belgian State (Federal Office for Scientific, Technical and Cultural Affairs). Most calculations have been performed at the Interuniversity Scientific Computing Facility (ISCF), set up at the Facultés Universitaires Notre-Dame de la Paix (Namur, Belgium), for which the authors gratefully acknowledge the financial support of the FNRS-FRFC and the "Loterie Nationale" for the convention n 2.4578.02, and the FUNDP.

Supporting Information Available: Benchmark calculations for the geometries of molecule **I** in Figure 2. This material is available free of charge via the Internet at http://pubs.acs.org.

References and Notes

(1) Brown, M. P.; Heseltine, R. W. *J. Inorg. Nucl. Chem.* **1967**, *29*, 1197−1201.
(2) In ref 1, the polymer actually synthesized is poly(methylaminoborane).
(3) Kwon, C. T. J.; McGee, H. A. *Inorg. Chem.* **1970**, *9*, 2458−2461.
(4) Komm, R.; Geanangel, R. A.; Liepins, R. *Inorg. Chem.* **1983**, *22*, 1684−1686.
(5) Kim, D. P.; Moon, K. T.; Kho, J. G.; Economy, J.; Gervais, C.; Babonneau, F. *Polym. Adv. Technol.* **1999**, *10*, 702−712.
(6) Gervais, C.; Babonneau, F. *J. Organomet. Chem.* **2002**, *657*, 75−82.
(7) Pustcioglu, S. Y.; McGee, H. A., Jr.; Fricke, A. L.; Hassler, J. C. *J. Appl. Polym. Sci.* **1977**, *21*, 1561−1567.
(8) Baitalow, F.; Baumann, J.; Wolf, G.; Jaenicke-Rössler, K.; Leitner, G. *Thermochim. Acta* **2002**, *391*, 159−168.
(9) Denton, D. L.; Johnson, A. D.; Hickam, C. W., Jr.; Bunting, R. K.; Shore, S. G. *J. Inorg. Nucl. Chem.* **1975**, 1037−1038.
(10) Geanangel, R. A.; Rabalais, J. W. *Inorg. Chem. Acta* **1985**, *97*, 59−64.
(11) Nöth, H.; Thomas, S. *Eur. J. Inorg. Chem.* **1999**, 1373−1379.
(12) Jaska, C. A.; Temple, K.; Lough, A. J.; Manners, I. *J. Am. Chem. Soc.* **2003**, *125*, 9424−9434.
(13) Jaska, C. A.; Temple, K.; Lough, A. J.; Manners, I. *Chem. Commun.* **2001**, 962−963.
(14) Jaska, C. A.; Manners, I. *J. Am. Chem. Soc.* **2004**, *126*, 2698−2699.
(15) Jaska, C. A.; Manners, I. *J. Am. Chem. Soc.* **2004**, *126*, 1334−1335.
(16) Abdurahman, A.; Albrecht, M.; Shukla, A.; Dolg, M. *J. Chem. Phys.* **1999**, *110*, 8819−8824.
(17) Nakhamnson, S. M.; Buongiorno Nardelli, M.; Bernholc, J. *Phys. Rev. Lett.* **2004**, *92*, 115504.
(18) Kormos, B. L.; Cramer, C. J. *Inorg. Chem.* **2003**, *42*, 6691−6700.
(19) Becke, A. D. *J. Chem. Phys.* **1993**, *98*, 5648.
(20) Schmider, H. L.; Becke, A. D. *J. Chem. Phys.* **1998**, *108*, 9624−9631.
(21) Adamo, C.; Barone, V. *J. Chem. Phys.* **1999**, *110*, 6158−6170.
(22) Frisch, M. J.; Trucks, G. W.; Schlegel, H. B.; Scuseria, G. E.; Robb, M. A.; Cheeseman, J. R.; Montgomery, J. A., Jr.; Vreven, T.; Kudin, K. N.; Burant, J. C.; Millam, J. M.; Iyengar, S. S.; Tomasi, J.; Barone, V.; Mennucci, B.; Cossi, M.; Scalmani, G.; Rega, N.; Petersson, G. A.; Nakatsuji, H.; Hada, M.; Ehara, M.; Toyota, K.; Fukuda, R.; Hasegawa, J.; Ishida, M.; Nakajima, T.; Honda, Y.; Kitao, O.; Nakai, H.; Klene, M.; Li, X.; Knox, J. E.; Hratchian, H. P.; Cross, J. B.; Adamo, C.; Jaramillo, J.; Gomperts, R.; Stratmann, R. E.; Yazyev, O.; Austin, A. J.; Cammi, R.; Pomelli, C.; Ochterski, J. W.; Ayala, P. Y.; Morokuma, K.; Voth, G. A.; Salvador, P.; Dannenberg, J. J.; Zakrzewski, V. G.; Dapprich, S.; Daniels, A. D.; Strain, M. C.; Farkas, O.; Malick, D. K.; Rabuck, A. D.; Raghavachari, K.; Foresman, J. B.; Ortiz, J. V.; Cui, Q.; Baboul, A. G.; Clifford, S.; Cioslowski, J.; Stefanov, B. B.; Liu, G.; Liashenko, A.; Piskorz, P.; Komaromi, I.; Martin, R. L.; Fox, D. J.; Keith, T.; Al-Laham, M. A.; Peng, C. Y.; Nanayakkara, A.; Challacombe, M.; Gill, P. M. W.; Johnson, B.; Chen, W.; Wong, M. W.; Gonzalez, C.; Pople, J. A. *Gaussian 03*, revision B.04; Gaussian, Inc.: Pittsburgh, PA, 2003.
(23) In this work, note that the extremities of the oligomers are NH_3/BH_3.
(24) Lebedev, V. I.; Skorokhodov, A. L. *Russ. Acad. Sci. Dokl. Math.* **1992**, *45*, 587−592.
(25) Quinet, O.; Champagne, B. *Int. J. Quantum Chem.* **2002**, *89*, 341−348.
(26) Scott, A. P.; Radom, L. *J. Phys. Chem.* **1996**, *100*, 16502−16513.
(27) Wong, M. W. *Chem. Phys. Lett.* **1996**, *256*, 391−399.
(28) Halls, M. D.; Schlegel, H. B. *J. Chem. Phys.* **1999**, *111*, 8819−8824.

(29) Halls, M. D.; Tripp, C. B.; Schlegel, H. B. *Phys. Chem. Chem. Phys.* **2001**, *3*, 2131−2136.
(30) Besler, B. H.; Merz, K. M.; Kollman, P. A. *J. Comput. Chem.* **1990**, *11*, 431−439.
(31) Sigfridsson, E.; Ryde, U. *J. Comput. Chem.* **1998**, *19*, 377−395.
(32) Breneman, C. M.; Wiberg, K. B. *J. Comput. Chem.* **1990**, *11*, 361−373.
(33) Runge, E.; Gross, E. K. U. *Phys. Rev. Lett.* **1984**, *52*, 997−1000.
(34) Cavillot, V.; Champagne, B. *Chem. Phys. Lett.* **2002**, *354*, 449−457.
(35) Baerends, E. J.; Ricciardi, G.; Rosa, A.; van Gisbergen, S. J. A. *Coord. Chem. Rev.* **2002**, *230*, 5−27.
(36) Jamorski-Jödicke, C.; Luthi, H. P. *J. Am. Chem. Soc.* **2002**, *125*, 252−264.
(37) Wilberg, K. B.; de Oliveria, A. E.; Trucks, G. *J. Phys. Chem. A* **2002**, *106*, 4192−4199.
(38) Infante, I.; Lelj, F. *Chem. Phys. Lett.* **2003**, *367*, 308−318.
(39) Jaworska, M.; Kazibut, G.; Lodowski, P. *J. Phys. Chem. A* **2003**, *107*, 1339−1347.
(40) Test geometry optimizations starting with a lower symmetry go back toward D_{2h}.
(41) Jagielska, A.; Moszynski, R.; Piela, L. *J. Chem. Phys.* **1999**, *110*, 947−954.
(42) Dillen, J.; Verhoeven, P. *J. Phys. Chem. A* **2003**, *107*, 2570−2577.
(43) Wilberg, K. B.; Stratmann, R. E.; Frisch, M. J. *Chem. Phys. Lett.* **1998**, *297*, 60−64.
(44) MP2/6-311G(2d) value. PBE0/6-31G(2d): 21.1°.
(45) Sun, H. *J. Am. Chem. Soc.* **1997**, *119*, 3611−3618.
(46) Jacquemin, D.; Lambert, C.; Perpète, E. A. *Macromolecules* **2004**, *37*, 1009−1015.
(47) Dorn, H.; Singh, R. A.; Massey, J.; Nelson, J. M.; Jaska, C. A.; Lough, A.; Manners, I. *J. Am. Chem. Soc.* **2000**, *122*, 6669−6678.
(48) Dorn, H.; Rodezno, J. M.; Brunnhofer, B.; Rivard, E.; Massey, J. A.; Manners, I. *Macromolecules* **2003**, *36*, 291−297.
(49) Starting from the three modes with an imaginary frequency, two structures have been obtained. The skeleton dihedral angles (in degrees, from NH_3 end to BH_3 end) found for structure 1 (2) are 28.2, 173.3, 37.2, 161.1, and −28.6 (29.7, 166.7, 54.6, −124.0, and 38.8) at the PBE0/6-31G(2d) level. The relative PBE0/6-31G(2d) energy per unit cell with regard to the trans−cisoid confomer are −0.43 and −1.04 kcal/mol, respectively.
(50) This phenomena seems typical of the PBE0 results. The MP2/6-311G(2d) helix does not display terminal coils.
(51) These six possible sequences are (1) 30 190 30 190 30, (2) 30 190 30 170 30, (3) 30 170 30 170 30, (4) 30 190 −30 190 30, (5) 30 190−30 170 30, and (6) 30 170 −30 170 30°.
(52) Different coils have been considered for the tetramer, and the values reported in the following are for the most stable structure. However, due to the large number of possibilities, we cannot fully guarantee that another coiled structure would not have been slightly more stable.
(53) For HEL chains, the BLA reverses sign between $N = 10$ and $N = 12$. Although the BLA is very close to zero in $N = 8-12$, it is difficult to assess quantitatively the polymeric BLA. However, as the bond lengths are almost constant between $N = 12$ and $N = 16$, one can predict a qualitatively small bond length alternation for extended oligomers.
(54) Reed, A. E.; Curtiss, L. A.; Weinhold, F. *Chem. Rev.* **1988**, *88*, 899−926.
(55) Perpète, E. A.; Champagne, B. *J. Mol. Struct.* (*THEOCHEM*) **1999**, *487*, 39−45.
(56) Klooster, W. T.; Koetzle, T. F.; Siegbahn, P. E. M.; Richardson, T. B.; Crabtree, R. H. *J. Am. Chem. Soc.* **1999**, *121*, 6337−6343.
(57) The experimental value is from: Smith et al. *J. Mol. Spectrosc.* **1973**, *45*, 327−373. The theoretical MP2/aug-cc-VDZ value is found in: Jagielska et al. *J. Chem. Phys.* **1999**, *110*, 947−954; 1333 cm^{-1}. Our scaled PBE0/6-31G(2d) value of 1324 cm^{-1} is in good agreement with both of them. For a complete discussion of the vibrational frequencies in gas-phase and solid-state borazane, see: Dillen et al. *J. Phys. Chem. A* **2003**, *107*, 2570−2577.
(58) Smith, J.; Seshardi, S.; White, D. *J. Mol. Spectrosc.* **1973**, *45*, 327−337.
(59) Using the PBE0/6-31G(2d) level and a 0.97 scaling factor.
(60) Gerry, M. C. L.; Lewis-Bevan, W.; Mere, A. J.; Westwood, N. P. C. *J. Mol. Spectrosc.* **1985**, *110*, 153−163.
(61) Widany, J.; Frauenheim, T.; Köhler, T.; Sternberg, M.; Porezag, D.; Jungnickel, G.; Seifert, G. *Phys. Rev. B* **1996**, *53*, 4443−4452.
(62) Böddeker, K. W.; Shore, S. G.; Bunting, R. K. *J. Am. Chem. Soc.* **1966**, *88*, 4396−4401.
(63) Jaska, C. A.; Lough, A. J.; Maners, I. *Inorg. Chem.* **2004**, *43*, 1090−1099.
(64) TT chains are bent due to the different steric and electronic properties of B−H and N−H bonds. This deviation from linearity of the backbone may explain the rough evolution of $\Delta\mu$.
(65) This 4 D value is a rough estimation as no clear converging pattern is observed for the $\Delta\mu(N)$ of long TT chains.
(66) From MP2/6-31G(d)//MP2/6-31G(d) calculations performed on the TC conformers of PP.
(67) Vračko, M.; Champagne, B.; Mosley, D.; André, J. M. *J. Chem. Phys.* **1995**, *102*, 6831−6836.
(68) Hirata, S.; Barlett, R. J. *J. Chem. Phys.* **2000**, *112*, 7339−7344.
(69) Ohno, M.; Zakrzewski, V. G.; Ortiz, J. V.; von Niessen, W. *J. Chem. Phys.* **1997**, *106*, 3258−3269.